Science Bulletin 67 (2022) 2162–2166

Contents lists available at ScienceDirect

Science Bulletin

journal homepage: www.elsevier.com/locate/scib

Article

Detection of spectral hardenings in cosmic-ray boron-to-carbon and boron-to-oxygen flux ratios with DAMPE

DAMPE Collaboration [1]

ARTICLE INFO

Article history:
Received 13 July 2022
Received in revised form 9 September 2022
Accepted 27 September 2022
Available online 14 October 2022

Keywords:
DAMPE
Commic-ray
CR propagation
B/C ratio
B/O ratio

ABSTRACT

Boron nuclei in cosmic rays (CRs) are believed to be mainly produced by the fragmentation of heavier nuclei, such as carbon and oxygen, via collisions with the interstellar matter. Therefore, the boron-to-carbon flux ratio (B/C) and the boron-to-oxygen flux ratio (B/O) are very essential probes of the CR propagation. The energy dependence of the B/C ratio from previous balloon-borne and space-based experiments can be well described by a single power-law up to about 1 TeV/n within uncertainties. This work reports direct measurements of B/C and B/O in the energy range from 10 GeV/n to 5.6 TeV/n with 6 years of data collected by the Dark Matter Particle Explorer, with high statistics and well controlled systematic uncertainties. The energy dependence of both the B/C and B/O ratios can be well fitted by a broken power-law model rather than a single power-law model, suggesting the existence in both flux ratios of a spectral hardening at about 100 GeV/n. The significance of the break is about 5.6σ and 6.9σ for the GEANT4 simulation, and 4.4σ and 6.9σ for the alternative FLUKA simulation, for B/C and B/O, respectively. These results deviate from the predictions of conventional turbulence theories of the interstellar medium (ISM), which point toward a change of turbulence properties of the ISM at different scales or novel propagation effects of CRs, and should be properly incorporated in the indirect detection of dark matter via anti-matter particles.

1. Introduction

Galactic cosmic rays (CRs) are energetic particles travelling through the interstellar space. They are messengers of the violent evolution of stars or stellar systems in extreme environments. CRs are typically divided into two classes, the primary and secondary families. Primary CRs are accelerated at astrophysical sources such as supernova remnants, while secondaries are produced from the interactions of the primaries with the interstellar medium (ISM) during the propagation [1,2]. The spectrum of accelerated particles at the source is expected to follow a power-law form $\mathscr{R}^{-p}$ according to the Fermi acceleration mechanism [3], where $\mathscr{R}$ is the rigidity and p is the power-law index. After the diffusive propagation in the ISM, the spectrum of primary CRs would soften to be $\propto \mathscr{R}^{-(p+\delta)}$, where δ is the slope of the rigidity-dependence of the diffusion coefficient. The parameter δ depends on the power spectrum of the turbulence of the ISM, with typical values of 1/3 for the Kolmogorov theory of interstellar turbulence [4] or 1/2 for the Kraichnan theory [5]. The spectrum of secondary CRs generated by the interaction of primary particles with the ISM is expected to be even softer, $\propto \mathscr{R}^{-(p+2\delta)}$. The flux ratio of the secondary-to-primary CRs is then $\propto \mathscr{R}^{-\delta}$, which sensitively depends on the propagation procedure. Precise measurements of the secondary-to-primary flux ratios are thus crucial to reliably constrain the propagation process of CRs [1,2].

Lithium, beryllium, and boron nuclei in CRs are dominantly produced by the fragmentation of heavier nuclei, since their primary abundances from stellar nucleosynthesis are many orders of magnitude lower than those of protons, helium, carbon, and oxygen. Among all the secondary-to-primary ratios, the B/C ratio is the most extensively measured. The B/O is in principle more directly related to the propagation procedure of CRs than B/C, due to that there is a small amount of secondary contribution for the carbon nuclei. Thanks to the contributions from worldwide experiments, the B/C ratio has been measured up to a few TeV/n [6–16], although the uncertainties are relatively large for kinetic energies above 500 GeV/n. A power-law decline form, $\propto \mathscr{R}^{-1/3}$, can well fit the rigidity (energy) dependence of the B/C ratio, in agreement with the prediction of the Kolmogorov turbulence [13]. Nevertheless, evidence of breaks of the secondary-to-primary flux ratios was shown by the AMS-02 measurements [15,16], though the break is not significant for individual B/C or B/O ratio. Improved measurements of the secondary-to-primary ratios, especially

---

[1] Members of DAMPE Collaboration are listed at the end of this paper.
E-mail address: dampe@pmo.ac.cn

https://doi.org/10.1016/j.scib.2022.10.002
2095-9273/

towards higher energies, are highly necessary to further understand the propagation of CRs and the properties of the ISM.

2. Results

In this work, we report the direct measurements of B/C and B/O with the DArk Matter Particle Explorer (DAMPE; also known as “Wukong”), a satellite-borne detector for high energy cosmic-ray and γ-ray observations [17]. The DAMPE payload consists of a Plastic Scintillator Detector (PSD) for the charge measurement, a Silicon Tungsten tracKer-converter (STK) for the trajectory reconstruction, a bismuth germanium oxide (BGO) imaging calorimeter for the energy measurement and electron–hadron discrimination, and a NeUtron Detector (NUD) to enhance electron–hadron separation [17,18]. With its relatively large geometric factor, good charge [19] and energy resolution [17], DAMPE is expected to extend the precise measurements of individual spectra of high-abundance CR species from protons to Iron nuclei up to a few hundreds of TeV energies [20,21]. The DAMPE satellite was launched into a 500-km Sun-synchronous orbit on 17 December 2015, and has operated stably in space since then, as illustrated by the on-orbit calibration [22].

The analysis presented in this work is based on the data recorded in the first 6 years of DAMPE’s operation, from January 1, 2016 to December 31, 2021. The live time fraction is about 75.85% after excluding the instrument dead time, the time for the on-orbit calibration, the time in the South Atlantic Anomaly (SAA) region, and the period between September 9, 2017 and September 13, 2017 during which a big solar flare affected the status of the detector [23]. The boron, carbon, and oxygen nuclei are efficiently identified based on the PSD charge measurement. Fig. 1 illustrates the reconstructed PSD charge distributions for events with $Z = 4 - 8$ and deposited energies in the calorimeter of 630 GeV to 2 TeV, and 3.16 TeV to 10 TeV. The Monte Carlo (MC) simulations for nuclei from beryllium to oxygen, generated with GEANT v4.10.05 [24], are shown by dashed lines to illustrate a best-fit to the flight data. Here, we suppress lighter nuclei ($Z < 4$) using a STK charge selection (see the Supplementary materials for details). Residual nuclei lighter than beryllium are too low to be shown in these plots.

The boron, carbon, and oxygen candidates are selected with energy-independent charges of [4.7, 5.3], [5.6, 6.4], and [7.6, 8.5], respectively. The total contamination of the boron sample is found to be $\sim 1\%$ for deposited energies around 100 GeV and $\sim 4.5\%$ around 50 TeV, while the contamination of the carbon and oxygen sample is $< 0.6\%$ and $< 1.6\%$ respectively, over the entire energy range. In Fig. 1, the distribution of MC oxygen shows a more prominent tail on the lower charge side compared with those from other nuclei, which is primarily due to their different fragmentation cross sections with the materials above or in the PSD. As a result, the contamination to boron from oxygen is larger than that from carbon. Similar distributions are also shown for the FLUKA [25] simulations, although the inelastic interactions of FLUKA and GEANT4 are different.

The selection efficiency and the energy response of the calorimeter are obtained with MC simulations, and validated from the flight data and the test beam data. Applying an unfolding procedure [26], we derive the B/C and B/O ratios in the energy range from 10 GeV/n to 5.6 TeV/n, as shown in Fig. 2 and tabulated in Table 1. The atomic mass numbers are assumed to be 10.7 (see Ref. [13]), 12, and 16 for boron, carbon, and oxygen, respectively. Compared with previous measurements by HEAO3 [6], CRN [7], ATIC-2 [9], CREAM-I [10], TRACER [11], PAMELA [12], AMS-02 [16], and NUCLEON [14], the DAMPE measurements are well consistent with them at low energies ($E_k \lesssim 500$ GeV/n) and improve the precision significantly at high energies. Particularly, the DAMPE results provide the first precise measurements of the B/C and B/O ratios above 1 TeV/n.

3. Discussion and conclusion

Fits to the DAMPE measurements show that both the energy dependence of B/C and B/O deviate from single power-law (PL) forms in the measured energy range. A broken power-law (BPL) model fit yields to a $\chi^2 = 6.61$ for 5 degrees of freedom (dof) while the PL fit yields to a $\chi^2 = 42.35$ for 7 dof for B/C, for the GEANT4 simulation. Similarly, for B/O, the BPL fit gives $\chi^2/\mathrm{dof} = 5.51/5$ while the PL fit yields $\chi^2/\mathrm{dof} = 57.81/7$. Therefore, the DAMPE data favor a spectral break of B/C (B/O) with a significance of 5.6σ (6.9σ) through comparing the $\Delta\chi^2$ values. The fits to the results with the FLUKA simulation give a significance of 4.4σ (6.9σ) for the B/C (B/O) ratio. The break energy is found to be $98.9^{+8.9+10.0}_{-8.8-0.0}$ ($99.5^{+7.4+7.7}_{-7.1-0.0}$) GeV/n, and the spectral indices below/above E_b are $(\gamma_1, \gamma_2) = (0.356^{+0.008+0.000}_{-0.008-0.017}, 0.201^{+0.024+0.008}_{-0.024-0.000})$ and $(\gamma_1, \gamma_2) = (0.394^{+0.010+0.000}_{-0.010-0.026}, 0.187^{+0.024+0.000}_{-0.024-0.019})$ for B/C and B/O, respectively (see the Supplementary materials for details). Here, the first error comes from the fitting and the second error comes from the

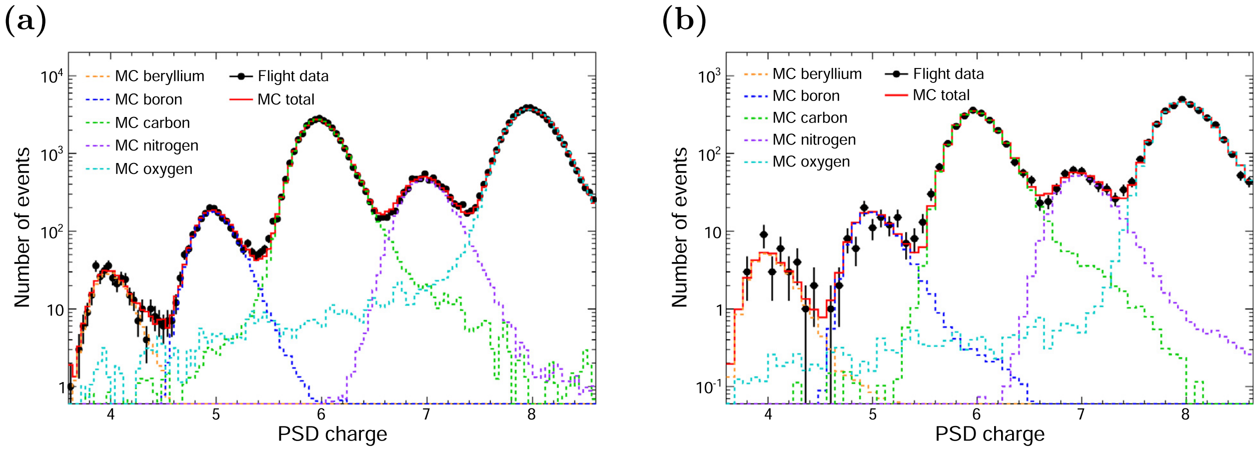

Fig. 1. The charge distributions measured by PSD for particles with $Z = 4 - 8$ and deposited energies in the calorimeter of 630 GeV to 2 TeV (a), and 3.16 TeV to 10 TeV (b). The flight data are shown by black dots. Dashed lines with different colors show the best-fit MC simulated samples of beryllium, boron, carbon, nitrogen, and oxygen nuclei. The sum of MC samples is shown by the red line.

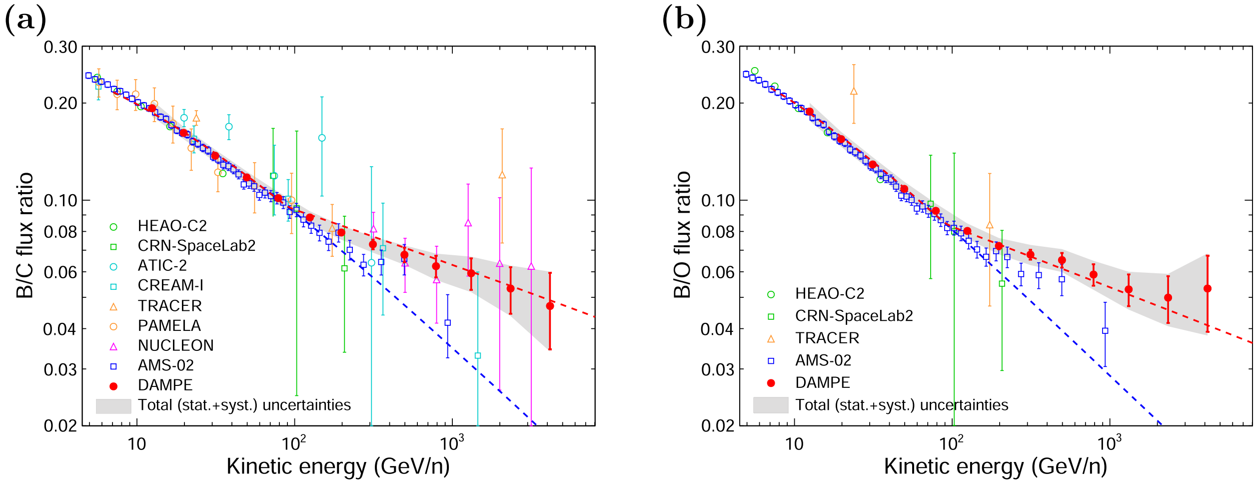

Fig. 2. Boron-to-carbon (a) and boron-to-oxygen (b) flux ratios as functions of kinetic energy per nucleon. DAMPE measurements are shown by red filled dots, with error bars and shaded bands representing the statistical and total uncertainties, respectively. The total uncertainties are the sum in quadrature of the statistical and systematic ones. The blue dashed lines show the fitting results for a GALPROP model with single power-law rigidity dependence of the diffusion coefficient, and the red dashed lines are the results with a hardening of the diffusion coefficient at 200 GV. In panel (a), other direct measurements by HEAO3 [6] (green circles), CRN [7] (green squares), ATIC-2 [9] (cyan circles), CREAM-I [10] (cyan squares), TRACER [11] (orange triangles), PAMELA [12] (orange circles), NUCLEON-KLEM [14] (magenta triangles) and AMS-02 [16] (blue squares) are shown for comparison. In panel (b), the measurements of B/O by HEAO3 [6] (green circles), CRN [7] (green squares), TRACER [11] (orange triangles) and AMS-02 [16] (blue squares) are shown. For the AMS-02 results [16], we convert the ratios from rigidity to kinetic energy per nucleon assuming an atomic mass number of 10.7 for boron, 12.0 for carbon, 16.0 for oxygen, and a power-law spectrum of carbon (oxygen) with an index of -2.6. The error bars of TRACER, CREAM-I, PAMELA, and AMS-02 data include both statistical and systematic uncertainties added in quadrature. For HEAO3, CRN, ATIC-2, and NUCLEON data only the statistical uncertainties are shown.

Table 1

Boron-to-carbon and boron-to-oxygen flux ratios measured with DAMPE, together with 1σ statistical and systematic uncertainties.

$\langle E\rangle$ (GeV/n)	E_{min} (GeV/n)	E_{max} (GeV/n)	B/C ratio $\pm\,\sigma_{\mathrm{stat}} \pm \sigma_{\mathrm{sys}}$	B/O ratio $\pm\,\sigma_{\mathrm{stat}} \pm \sigma_{\mathrm{sys}}$
12.5	10.0	15.8	$0.1926 \pm 0.0017 \pm 0.0111$	$0.1882 \pm 0.0025 \pm 0.0119$
19.8	15.8	25.1	$0.1616 \pm 0.0007 \pm 0.0070$	$0.1546 \pm 0.0008 \pm 0.0081$
31.3	25.1	39.8	$0.1373 \pm 0.0006 \pm 0.0061$	$0.1290 \pm 0.0007 \pm 0.0068$
49.7	39.8	63.1	$0.1176 \pm 0.0007 \pm 0.0051$	$0.1084 \pm 0.0008 \pm 0.0057$
78.7	63.1	100	$0.1015 \pm 0.0010 \pm 0.0044$	$0.0927 \pm 0.0010 \pm 0.0049$
125	100	158	$0.0884 \pm 0.0013 \pm 0.0038$	$0.0803 \pm 0.0012 \pm 0.0042$
198	158	251	$0.0794 \pm 0.0018 \pm 0.0036$	$0.0722 \pm 0.0017 \pm 0.0038$
313	251	398	$0.0730 \pm 0.0025 \pm 0.0033$	$0.0678 \pm 0.0024 \pm 0.0043$
497	398	631	$0.0678 \pm 0.0035 \pm 0.0031$	$0.0652 \pm 0.0034 \pm 0.0041$
787	631	1000	$0.0624 \pm 0.0048 \pm 0.0034$	$0.0588 \pm 0.0045 \pm 0.0041$
1315	1000	1778	$0.0594 \pm 0.0067 \pm 0.0034$	$0.0529 \pm 0.0059 \pm 0.0039$
2339	1778	3162	$0.0532 \pm 0.0088 \pm 0.0036$	$0.0499 \pm 0.0083 \pm 0.0041$
4160	3162	5623	$0.0470 \pm 0.0125 \pm 0.0038$	$0.0532 \pm 0.0141 \pm 0.0055$

comparison with the alternative analysis based on the FLUKA simulation. We find that the break energies and the high-energy spectral indices of B/C and B/O are consistent with each other, while the low-energy spectral index of B/C is slightly harder than that of B/O. The difference may come from the fact that the carbon spectrum is softer than the oxygen spectrum below $\sim$ 100 GeV/n as revealed by AMS-02 [16] and CALET [27], which may be due to a small secondary contribution of carbon from oxygen and heavier nuclei. The corresponding spectral index changes are found to be $\Delta\gamma = 0.155^{+0.026+0.000}_{-0.026-0.026}$ ($\Delta\gamma = 0.207^{+0.027+0.000}_{-0.028-0.007}$) for B/C (B/O).

The DAMPE results have far-reaching implications on the propagation of Galactic CRs. The slope parameter δ of the diffusion coefficient is predicted to be either 1/3 or 1/2 in the conventional turbulence theories [4,5]. The detection of spectral hardenings in the B/C and B/O ratios by DAMPE thus challenges these conventional scenarios. To introduce a spectral break of the diffusion coefficient may be the simplest solution to account for the observations [28]. We have illustrated in Fig. 2 that the fitting to the pre-DAMPE data with a single power-law form of the diffusion coefficient, $D(R) \propto R^{\delta}$ with $\delta = 0.477$ [29], using the GALPROP model [30] assuming the convective transportation of CRs, deviates clearly from the DAMPE high-energy measurements (see the blue dashed lines). If we add a spectral break at $R_{\mathrm{br}} = 200$ GV, with a high-energy slope $\delta_h = 0.2$, the model prediction matches well with the measurements as shown by the red dashed lines. Intriguingly, the inferred $\delta = 0.477$ at rigidities of $\leqslant$ 200 GV is very close to the prediction of the Kraichnan theory of turbulence [5]. At higher rigidities, the rigidity dependence of $R^{-0.2}$ is harder than that expected by the Kolmogorov theory of turbulence [4]. This deviation may be relieved if a small amount of secondary particles were generated at the sources (i.e., they experience the same propagation process and thus give rise to a constant, although small, ratio). Our findings may thus imply the change of turbulence properties of the ISM at different scales, e.g., from the magnetized turbulence (Kraichnan type) at smaller scales to isotropic, stationary hydrodynamic turbulence (Kolmogorov type) at larger scales.

Alternatively, more complicated propagation or acceleration effects of CRs may also result in hardenings of the secondary-to-primary ratios. These models include, but are not limited to, the nested leaky box propagation model with different energy-dependence of the residence time in the ISM and the cocoon regions surrounding the sources [31], the production and acceleration of secondary particles at sources [32], the re-acceleration of CRs by random magnetohydrodynamic waves during the propagation [29] or by a local shock [33], the self-generation of turbulence by CRs [34], the spatially-dependent diffusion of particles [35], or possibly, a mixture of some of them [36].

In addition to the CR propagation studies, a significant spectral hardening of B/C (B/O) should be properly addressed in the search of dark matter annihilation or decay products with the antiparticle CRs, such as positrons and antiprotons, since the predictions of astrophysical background and the dark matter induced signal should both be affected by the change of the diffusion process. For instance, the previously claimed excess in the anti-proton data [37,38] may need a thorough re-examination to critically address its potential connection with the dark matter annihilation or decay. Improved measurements of the B/C, B/O, and other secondary-to-primary ratios with higher statistics and lower systematics by DAMPE and future direct detection experiments such as HERD [39], AMS-100 [40], and ALADInO [41] are expected to eventually uncover the fundamental problems of the origin and propagation of CRs and shed new light on the indirect detection of dark matter particles.

Conflict of interest

The authors declare that they have no conflict of interest.

Acknowledgments

The DAMPE mission was funded by the Strategic Priority Science and Technology Projects in Space Science of Chinese Academy of Sciences (CAS). In China, the data analysis was supported by the National Natural Science Foundation of China (11921003, 11903084, 12003076, 12022503, 12103094, and 12220101003), the Strategic Priority Science and Technology Projects of CAS (XDA15051100), the CAS Project for Young Scientists in Basic Research (YSBR-061), the Youth Innovation Promotion Association of CAS, the Natural Science Foundation of Jiangsu Province (BK20201107), and the Program for Innovative Talents and Entrepreneur in Jiangsu. In Europe, the activities and data analysis were supported by the Swiss National Science Foundation (SNSF), Switzerland, the National Institute for Nuclear Physics (INFN), Italy, and the European Research Council (ERC) under the European Unions Horizon 2020 research and innovation programme (851103).

Appendix A. Supplementary materials

Supplementary materials to this article can be found online at https://doi.org/10.1016/j.scib.2022.10.002.

References

[1] Strong AW, Moskalenko IV, Ptuskin VS. Cosmic-ray propagation and interactions in the Galaxy. Annu Rev Nucl Part S 2007;57:285.
[2] Becker Tjus J, Merten L. Closing in on the origin of Galactic cosmic rays using multimessenger information. Phys Rep 2020;872:1.
[3] Fermi E. On the origin of the cosmic radiation. Phys Rev 1949;75:1169.
[4] Kolmogorov A. The local structure of turbulence in incompressible viscous fluid for very large Reynolds' numbers. Akademiia Nauk SSSR Doklady 1941;30:301.
[5] Kraichnan RH. Inertial-range spectrum of hydromagnetic turbulence. Phys Fluids 1965;8:1385.
[6] Engelmann JJ, Ferrando P, Soutoul A, et al. Charge composition and energy spectra of cosmic-ray nuclei for elements from Be to Ni - Results from HEAO-3-C2. Astron Astrophys 1990;233:96.
[7] Swordy SP, Mueller D, Meyer P, et al. Relative bundances of secondary and primary cosmic rays at high energies. Astrophys J 1990;349:625.
[8] AMS Collaboration, Aguilar M, et al. Relative composition and energy spectra of light nuclei in cosmic rays: results from AMS-01. Astrophys J 2010;724:329.
[9] Panov AD, Sokolskaya NV, Adams JH, et al. Relative abundances of cosmic ray nuclei B-C-N-O in the energy region from 10 GeV/n to 300 GeV/n. Results from ATIC-2 (the science flight of ATIC). Int Cosmic Ray Conf 2008;2:3.
[10] Ahn HS, Allison PS, Bagliesie MG, et al. Measurements of cosmic-ray secondary nuclei at high energies with the first flight of the CREAM balloon-borne experiment. Astropart Phys 2008;30:133.
[11] Obermeier A, Ave M, Boyle P, et al. Energy spectra of primary and secondary cosmic-ray nuclei measured with TRACER. Astrophys J 2011;742:14.
[12] Adriani O, Barbarino GC, Bazilevskaya GA, et al. Measurement of boron and carbon fluxes in cosmic rays with the PAMELA experiment. Astrophys J 2014;791:93.
[13] AMS Collaboration, Aguilar M, et al. Precision measurement of the boron to carbon flux ratio in cosmic rays from 1.9 GV to 2.6 TV with the Alpha Magnetic Spectrometer on the International Space Station. Phys Rev Lett 2016;117:231102.
[14] Grebenyuk V, Karmanov D, Kovalev I, et al. Secondary cosmic rays in the NUCLEON space experiment. Adv Space Res 2019;64:2559.
[15] AMS Collaboration, Aguilar M, et al. Observation of new properties of secondary cosmic rays lithium, beryllium, and boron by the Alpha Magnetic Spectrometer on the International Space Station. Phys Rev Lett 2018;120:021101.
[16] AMS Collaboration, Aguilar M, et al. The Alpha Magnetic Spectrometer (AMS) on the International Space Station: Part II - results from the first seven years. Phys Rep 2021;894:1.
[17] Chang J, Ambrosi G, An Q, et al. The DArk Matter Particle Explorer mission. Astropart Phys 2017;95:6.
[18] DAMPE Collaboration, Ambrosi G, et al. Direct detection of a break in the teraelectronvolt cosmic-ray spectrum of electrons and positrons. Nature 2017;552:63.
[19] Dong T-K, Zhang Y-P, Ma P-X, et al. Charge measurement of cosmic ray nuclei with the plastic scintillator detector of DAMPE. Astropart Phys 2019;105:31.
[20] DAMPE Collaboration, An Q, et al. Measurement of the cosmic ray proton spectrum from 40 GeV to 100 TeV with the DAMPE satellite. Sci Adv 2019;5:eaax3793.
[21] DAMPE Collaboration, Alemanno F, et al. Measurement of the cosmic ray helium energy spectrum from 70 GeV to 80 TeV with the DAMPE space mission. Phys Rev Lett 2021;126:201102.
[22] Ambrosi G, An Q, Asfandiyarov R, et al. The on-orbit calibration of DArk Matter Particle Explorer. Astropart Phys 2019;106:18.
[23] DAMPE Collaboration, Alemanno F, et al. Observations of forbush decreases of cosmic-ray electrons and positrons with the DArk Matter Particle Explorer. Astrophys J Lett 2021;920:L43.
[24] Geant4 Collaboration, Agostinelli C, et al. GEANT4–a simulation toolkit. Nucl Instrum Meth A 2003;506:250.
[25] Böhlen TT, Cerutti F, Chin MPW, et al. The FLUKA code: developments and challenges for high energy and medical applications. Nucl Data Sheets 2014;120:211.
[26] D'Agostini G. A multidimensional unfolding method based on Bayes' theorem. Nucl Instrum Meth A 1995;362:487.
[27] CALET Collaboration, Adriani O, et al. Direct measurement of the cosmic-ray carbon and oxygen spectra from 10 GeV/n to 2.2 TeV/n with the Calorimetric Electron Telescope on the International Space Station. Phys Rev Lett 2020;125:251102.
[28] Génolini Y, Serpico PD, Boudaud M, et al. Indications for a high-rigidity break in the cosmic-ray diffusion coefficient. Phys Rev Lett 2017;119:241101.
[29] Yuan Q, Zhu C-R, Bi XJ, et al. Secondary cosmic-ray nucleus spectra disfavor particle transport in the Galaxy without reacceleration. J Cos Astropart Phys 2020;11:027.
[30] Strong AW, Moskalenko IV. Propagation of cosmic-ray nucleons in the Galaxy. Astrophys J 1998;509:212.
[31] Cowsik R, Madziwa-Nussinov R. Spectral intensities of antiprotons and the nested leaky-box model for cosmic rays in the Galaxy. Astrophys J 2016;827:119.
[32] Mertsch P, Vittino A, Sarkar S. Explaining cosmic ray antimatter with secondaries from old supernova remnants. Phys Rev D 2021;104:103029.
[33] Malkov MA, Moskalenko IV. On the origin of observed cosmic-ray spectrum below 100 TV. Astrophys J 2022;933:78.
[34] Blasi P, Amato E, Serpico PD. Spectral breaks as a signature of cosmic ray induced turbulence in the Galaxy. Phys Rev Lett 2012;109:061101.
[35] Tomassetti N. Origin of the cosmic-ray spectral hardening. Astrophys J Lett 2012;752:L13.
[36] Bresci V, Amato E, Blasi P, et al. Effects of re-acceleration and source grammage on secondary cosmic rays spectra. Mon Not Roy Astron Soc 2019;488:2068.
[37] Cui M-Y, Yuan Q, Tsai SYL, et al. Possible dark matter annihilation signal in the AMS-02 antiproton data. Phys Rev Lett 2017;118:191101.
[38] Cuoco A, Krämer M, Korsmeier M. Novel dark matter constraints from antiprotons in light of AMS-02. Phys Rev Lett 2017;118:191102.
[39] HERD Collaboration, Zhang S-N, et al. The high energy cosmic-radiation detection (HERD) facility onboard China's Space Station. Proc SPIE 2014;9144:91440X.
[40] Schael S, Atanasyan A, Berdugo J, et al. AMS-100: the next generation magnetic spectrometer in space – An international science platform for physics andastrophysics at Lagrange point 2. Nucl Instrum Meth A 2019;944:162561.
[41] Adriani O, Altomare C, Ambrosi G, et al. Design of an antimatter large acceptance detector in orbit (ALADInO). Instruments 2022;6:19.

The DAMPE experiment

The DAMPE is the first Chinese astronomical satellite, which consists of four sub-detectors, including the plastic scintillator detector, the silicon tracker, the BGO calorimeter and the neutron detector. As a general-purpose high-energy cosmic ray and gamma-ray detector, DAMPE is distinguished by the unprecedented high energy resolution on measuring the cosmic ray electrons and gamma-rays. The main scientific objectives addressed by DAMPE include probing the dark matter via the detection of high-energy electrons/positrons and gamma-rays, understanding the origin, acceleration, and propagation of cosmic rays in the Milky Way, and studying the gamma-ray astronomy. The DAMPE mission is funded by the Strategic Priority Science and Technology Projects in Space Science of the Chinese Academy of Sciences. The DAMPE Collaboration consists of more than 150 members from 3 countries, including physicists, astrophysicists, and engineers.

DAMPE collaboration

Francesca Alemanno[a,b], Corrado Altomare[c], Qi An[d,e], Philipp Azzarello[f], Felicia Carla Tiziana Barbato[a,b], Paolo Bernardini[g,h], Xiao-Jun Bi[i,j], Ming-Sheng Cai[k,l], Elisabetta Casilli[g,h], Enrico Catanzani[m], Jin Chang[k,l], Deng-Yi Chen[k], Jun-Ling Chen[n], Zhan-Fang Chen[k,l], Ming-Yang Cui[k], Tian-Shu Cui[o], Yu-Xin Cui[k,l], Hao-Ting Dai[d,e], Antonio De Benedittis[g,h][2], Ivan De Mitri[a,b], Francesco de Palma[g,h], Maksym Deliyergiyev[f], Adriano Di Giovanni[a,b], Margherita Di Santo[a,b], Qi Ding[k,l], Tie-Kuang Dong[k], Zhen-Xing Dong[o], Giacinto Donvito[c], David Droz[f], Jing-Lai Duan[n], Kai-Kai Duan[k], Domenico D'Urso[m][3], Rui-Rui Fan[j], Yi-Zhong Fan[k,l], Fang Fang[n], Kun Fang[j], Chang-Qing Feng[d,e], Lei Feng[k], Mateo Fernandez Alonso[a,b], Jennifer Maria Frieden[f][4], Piergiorgio Fusco[c,p], Min Gao[j], Fabio Gargano[c], Ke Gong[j], Yi-Zhong Gong[k], Dong-Ya Guo[j], Jian–Hua Guo[k,l], Shuang-Xue Han[o], Yi-Ming Hu[k], Guang-Shun Huang[d,e], Xiao-Yuan Huang[k,l], Yong-Yi Huang[k], Maria Ionica[m], Lu-Yao Jiang[k], Wei Jiang[k], Jie Kong[n], Andrii Kotenko[f], Dimitrios Kyratzis[a,b], Shi-Jun Lei[k], Wei-Liang Li[o], Wen–Hao Li[k,l], Xiang Li[k,l], Xian-Qiang Li[o], Yao-Ming Liang[o], Cheng-Ming Liu[d,e], Hao Liu[k], Jie Liu[n], Shu-Bin Liu[d,e], Yang Liu[k], Francesco Loparco[c,p], Chuan-Ning Luo[k,l], Miao Ma[o], Peng-Xiong Ma[k], Tao Ma[k], Xiao-Yong Ma[o], Giovanni Marsella[g,h][5], Mario Nicola Mazziotta[c], Dan Mo[n], Maria Muñoz Salinas[f], Xiao-Yang Niu[n], Xu Pan[k,l], Andrea Parenti[a,b], Wen-Xi Peng[j], Xiao-Yan Peng[k], Chiara Perrina[f][6], Enzo Puti-Garcia[f], Rui Qiao[j], Jia-Ning Rao[o], Arshia Ruina[f], Zhi Shangguan[o], Wei-Hua Shen[o], Zhao-Qiang Shen[k], Zhong-Tao Shen[d,e], Leandro Silveri[a,b], Jing-Xing Song[o], Mikhail Stolpovskiy[f], Hong Su[n], Meng Su[q], Hao-Ran Sun[d,e], Zhi-Yu Sun[n], Antonio Surdo[h], Xue-Jian Teng[o], Andrii Tykhonov[f], Jin-Zhou Wang[j], Lian-Guo Wang[o], Shen Wang[k], Shu-Xin Wang[k,l], Xiao-Lian Wang[d,e], Yan-Fang Wang[d,e], Ying Wang[d,e], Yuan-Zhu Wang[k], Da-Ming Wei[k,l], Jia-Ju Wei[k], Yi-Feng Wei[d,e], Di Wu[j], Jian Wu[k,l], Li-Bo Wu[a,b], Sha-Sha Wu[o], Xin Wu[f], Zi-Qing Xia[k], En–Heng Xu[d,e], Hai-Tao Xu[o], Jing Xu[k], Zhi-Hui Xu[k,l], Zi-Zong Xu[d,e], Zun-Lei Xu[k], Guo-Feng Xue[o], Hai-Bo Yang[n], Peng Yang[n], Ya-Qing Yang[n], Hui-Jun Yao[n], Yu-Hong Yu[n], Guan-Wen Yuan[k,l], Qiang Yuan[k,l], Chuan Yue[k], Jing-Jing Zang[k][7], Sheng-Xia Zhang[n], Wen-Zhang Zhang[o], Yan Zhang[k], Ya-Peng Zhang[n], Yi Zhang[k,l], Yong-Jie Zhang[n], Yong-Qiang Zhang[k], Yun-Long Zhang[d,e], Zhe Zhang[k], Zhi-Yong Zhang[d,e], Cong Zhao[d,e], Hong-Yun Zhao[n], Xun-Feng Zhao[o], Chang-Yi Zhou[o], and Yan Zhu[o]

[a]Gran Sasso Science Institute (GSSI), I-67100 L'Aquila, Italy.

[b]Istituto Nazionale di Fisica Nucleare (INFN) - Laboratori Nazionali del Gran Sasso, I-67100 Assergi, L'Aquila, Italy.

[c]Istituto Nazionale di Fisica Nucleare, Sezione di Bari, I-70126 Bari, Italy.

[d]State Key Laboratory of Particle Detection and Electronics, University of Science and Technology of China, Hefei 230026, China.

[e]Department of Modern Physics, University of Science and Technology of China, Hefei 230026, China.

[f]Department of Nuclear and Particle Physics, University of Geneva, CH-1211, Switzerland.

[g]Dipartimento di Matematica e Fisica E. De Giorgi, Università del Salento, I-73100, Lecce, Italy.

[h]Istituto Nazionale di Fisica Nucleare (INFN) - Sezione di Lecce, I-73100, Lecce, Italy.

[i]University of Chinese Academy of Sciences, Beijing 100049, China.

[j]Particle Astrophysics Division, Institute of High Energy Physics, Chinese Academy of Sciences, Beijing 100049, China.

[k]Key Laboratory of Dark Matter and Space Astronomy, Purple Mountain Observatory, Chinese Academy of Sciences, Nanjing 210023, China.

[l]School of Astronomy and Space Science, University of Science and Technology of China, Hefei 230026, China.

[m]Istituto Nazionale di Fisica Nucleare (INFN) - Sezione di Perugia, I-06123 Perugia, Italy.

[n]Institute of Modern Physics, Chinese Academy of Sciences, Lanzhou 730000, China.

[o]National Space Science Center, Chinese Academy of Sciences, Beijing 100190, China.

[p]Dipartimento di Fisica "M. Merlin", dell'Università e del Politecnico di Bari, I-70126 Bari, Italy.

[q]Department of Physics and Laboratory for Space Research, the University of Hong Kong, Hong Kong, China.

---

[2] Now at Istituto Nazionale Fisica Nucleare (INFN), Sezione di Napoli, IT-80126 Napoli, Italy.

[3] Now at Università di Sassari, Dipartimento di Chimica e Farmacia, I-07100, Sassari, Italy.

[4] Also at Institute of Physics, Ecole Polytechnique Fédérale de Lausanne (EPFL), CH-1015 Lausanne, Switzerland.

[5] Now at Dipartimento di Fisica e Chimica "E. Segrè", Università degli Studi di Palermo, I-90128 Palermo, Italy.

[6] Also at Institute of Physics, Ecole Polytechnique Fédérale de Lausanne (EPFL), CH-1015 Lausanne, Switzerland.

[7] Also at School of Physics and Electronic Engineering, Linyi University, Linyi 276000, China.